**Phthalocyanines**
**Фталоцианины**

Макрогетероциклы
http://macroheterocycles.isuct.ru

**Review**
**Обзор**

# Core−Modified Phthalocyanines and Subphthalocyanines: a Synthetic Strategy towards Core−Modification and Novel Properties Arising from the Inner Ring−Expansion

Soji Shimizu,[a,b@1] and Hiroyuki Furuta[a,b@2]

[a]*Department of Chemistry and Biochemistry, Graduate School of Engineering, Kyushu University, 819-0395 Fukuoka, Japan*
[b]*Center for Molecular Systems (CMS), 819-0395 Fukuoka, Japan*
[@1]*Corresponding author E-mail: ssoji@cstf.kyushu-u.ac.jp*
[@2]*Corresponding author E-mail: hfuruta@cstf.kyushu-u.ac.jp*

*This microreview covers contribution of the authors in the synthesis of novel "core-modified phthalocyanines and subphthalocyanines" bearing a larger ring unit than a five-membered pyrrole ring in the core. The core-modification does not only cause structural deformation, but also causes significant changes in the optical and electrochemical properties.*

**Keywords:** Phthalocyanine, subphthalocyanine, core-modification, aromaticity.

# Модифицированные фталоцианины и субфталоцианины: синтетическая стратегия модификации макроцикла и новые свойства, возникающие при расширении внутреннего кольца

С. Шимизу,[a,b@1] Х. Фурута[a,b@2]

[a]*Департамент химии и биохимии, Высшая школа инженерных наук, Университет Кюсю, 819-0395 Фукуока, Япония*
[b]*Центр молекулярных систем, 819-0395 Фукуока, Япония*
[@1]*E-mail: ssoji@cstf.kyushu-u.ac.jp*
[@2]*E-mail: hfuruta@cstf.kyushu-u.ac.jp*

*В обзоре описан вклад авторов в синтез новых модифицированных фталоцианинов и субфталоцианинов на основе более широких, чем пятичленное пиррольное кольцо, циклов. Модификация ядра не только вызывает структурную деформацию, но и является причиной значительных изменений оптических и электрохимических свойств.*

**Ключевые слова:** Фталоцианин, субфталоцианин, модификация координационной полости, ароматичность.

## Introduction

Phthalocyanines (Pcs) have been one of the indispensable functional dyes and pigments in industry since its serendipitous discovery in the early 1900s (Figure 1),[1] and they have been utilized in a variety of industrial and medical applications, such as catalysts, deodorants, optical discs, photodynamic therapy, semiconductors, solar cells, nonlinear optics and so forth.[2-5] The unique optical and electrochemical properties of these blue and green compounds originate from the aromatic 18π-electron conjugated system consisting of four isoindole rings bridged by four imino nitrogen atoms at the *meso*-positions. As it has been demonstrated in the chemistry of porphyrin (Figure 1), which is a similar to 18 π-electron conjugated pyrrole-containing macrocycle with methine carbon bridges at *meso*-positions, core-modification including

expansion of the inner pyrrolic rings or replacement of the pyrrolic rings with other heteroaromatic ring units, such as furan and thiophene, is an effective synthetic strategy to modify the optical and electrochemical properties as well as the coordination ability (Figure 2).[6]
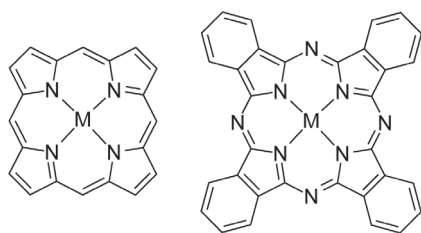


**Figure 1.** Structures of porphyrin (left) and phthalocyanine (right).



X = O, S, Se, Te, P
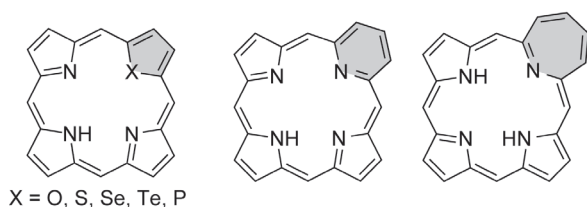
**Figure 2.** Representative examples of core-modified porphyrins.

In the phthalocyanine chemistry, hemiporphyrazines have been known as a class of core-modified phthalocyanine (Pc) analogues (Figure 3).[7-9] Despite their facile synthesis from a mixed condensation of 1,3-diiminoisoindoline and
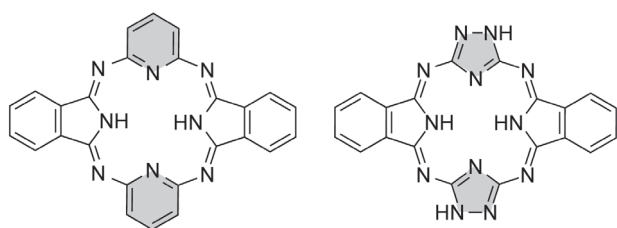


**Figure 3.** Representative examples of hemiporphyrazines.

heteroaromatic diamines, in most cases hemiporphyrazines exhibit totally different nonaromatic characters because the local conjugation of the heteroaromatic ring units is dominant over the macrocyclic conjugated system. Therefore, core-modification with maintaining Pc-like aromatic characters has remained challenging in the chemistry of Pc despite the expectation of drastic changes in the optical and electrochemical properties upon core-modification.

Considering that the inner pyrrolic rings are formed by a reaction of nitrile groups of *o*-phthalonitrile with a 1,2-relationship, we have attempted to use dinitrile derivatives bearing nitrile groups with a 1,3- or 1,4-relationship to create a six- or seven-membered ring unit in the core of Pc (Figure 4). Using 1,8-naphthalenedicarbonitrile and 2,2'-biphenyldicarbonitrile as key precursors, core-modified Pc analogues with six- and seven-membered ring units, which retained Pc-like macrocyclic conjugated systems, were successfully synthesized.[10,11] By applying this synthetic strategy to subphthalocyanine (SubPc), which is a ring contracted Pc analogue, core-modified SubPc analogues were also synthesized.[12-14] In this microreview, the contribution of the authors in the synthesis of core-modified Pcs and SubPcs as well as the their unique properties arising from the core-modification are surveyed.

## Core-Modified Pcs

Core-modification based on the above-mentioned strategy was initially achieved in our group using 1,8-naphthalenedicarbonitrile[15] as a precursor.[10,16] A mixed condensation reaction with *o*-phthalonitrile in the presence of nickel acetate and hydroquinone, and in the absence of solvent at 300 °C has provided core-modified Pcs with a six-membered ring embedded in an azaphenalene unit, which is therefore referred to as azaphenalenephthalocyanine (APPc) (Scheme 1, conditions a). In addition to Pc **1a** and APPc **2a** obtained in the yields of 9 and 26 %, respectively, disubstituted species with adjacently arranged azaphenalene units (*adj*-AP₂Pc, **3**) were also obtained in 13 % yield. The absence of the disubstituted species with oppositely arranged azaphenalene units (*opp*-AP₂Pc, **4**) could be due to preferential formation of diisoindole and/or diazaphenalene half-Pc intermediates at the solid-state reaction. After several attempts to obtain **4**, we have found that a mixed condensation reaction of the
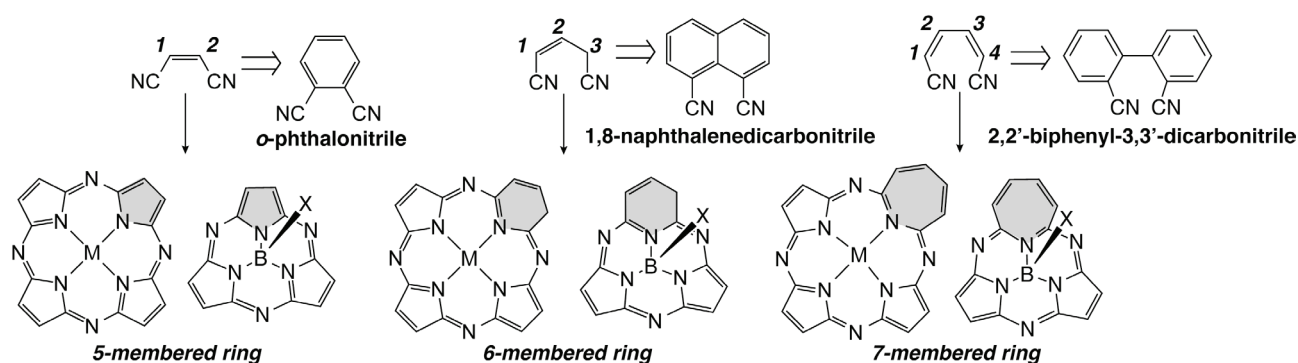


**Figure 4.** Strategy towards core-modification of Pc and SubPc.
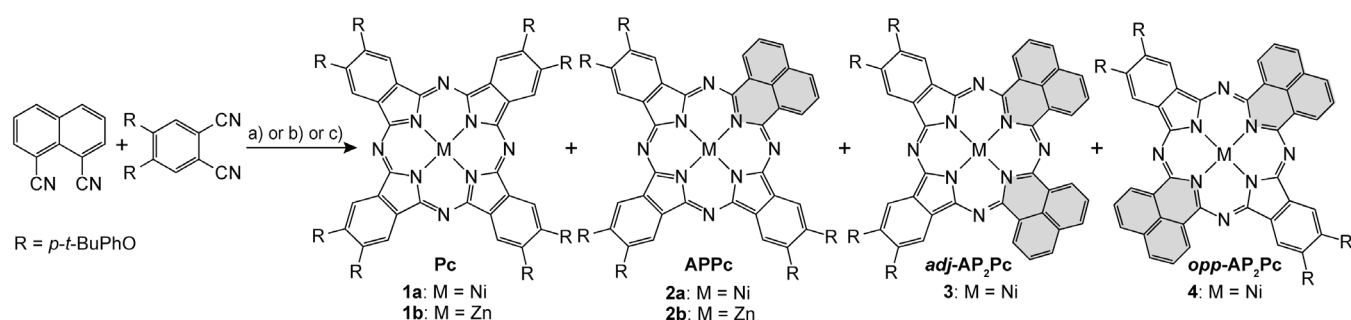
**Scheme 1.** Synthesis of azaphenalenephthalocyanines (APPcs). Conditions: a) Ni(OAc)$_2$, hydroquinone, 300 °C, 15 min. b) Ni(OAc)$_2$, (NH$_4$)$_2$MoO$_4$, quinoline, 330 °C, 15 min. c) Zn(OAc)$_2$, hydroquinone, 260 °C, 20 min.

two dinitrile precursors and nickel acetate in the presence of ammonium molybdate in quinoline at 330 °C has successfully provided **1a**, **2a**, **3**, and **4** in 11, 30, 15 and 1.4 % yield, respectively (Scheme 1, conditions b). As a metal template, zinc acetate could also be utilized under solvent-free reaction conditions at the lower reaction temperature of 260 °C, but in this case only zinc complex of APPc **2b** was obtained (Scheme 1, conditions c).

In order to further expand the inner ring unit from a six-membered ring to a seven-membered ring, 2,2'-biphenyldi-carbonitrile[17] bearing nitrile groups with a 1,4-relationship was used. Under similar solution-state reaction conditions performed for the synthesis of APPc and its analogues (APPcs), a seven-membered ring was successfully incorporated into the structure of Pc as an azepine ring (Scheme 2).[11a] This core-modified Pc with the largest inner ring units is referred to as azepiphthalocyanine (AZPPc, **5a** and **5b**). In this case, only a mono-substituted Pc analogue was obtained

probably due to the severe steric effect of the large seven-membered ring unit. Other dinitrile derivatives, such as 2,2'-bipyridyl-3,3'-dicarbonitrile and 4,5-phenanthrenedi-carbonitrile[17,18] can also be utilized in place of 2,2'-biphe-nyldicarbonitrile to provide seven-membered ring-containing species **6** and **7**, respectively (Scheme 2).[11b]

Based on the X-ray crystallographic analysis and DFT calculations, a structural deformation caused by the expansion of the inner ring unit was revealed.[10,11] The crystal structure of APPc **2b** has exhibited a rather planar structure with a pyridine axial ligand, in which the azaphenalene unit was slightly tilted by 3.3° from the mean plane of the four zinc-coordinating nitrogen atoms (4N mean plane) (Figure 5). The central zinc ion was deviated by 0.33 Å from the 4N mean plane. Since growing single crystals of nickel complexes, **2a**, **3**, and **4**, was unsuccessful, DFT calculations were performed to give insights into their structures (Figure 6). In contrast to the planar structure of **2b**, the optimized structure of **2a** has
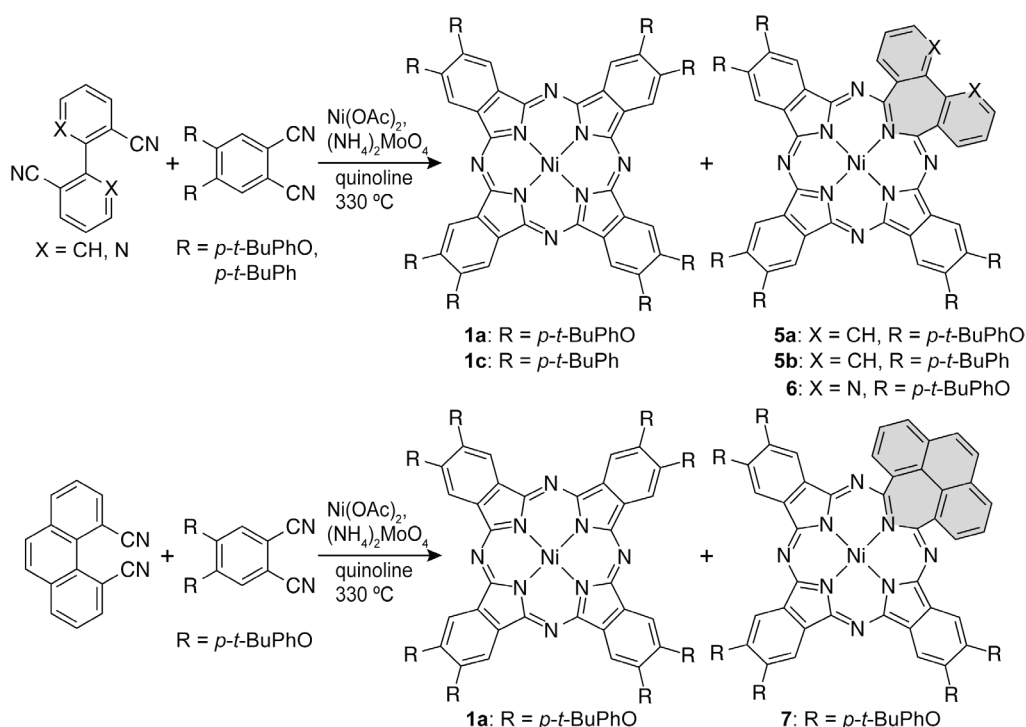


**Scheme 2.** Synthesis of the azepiphthalocyanines series.
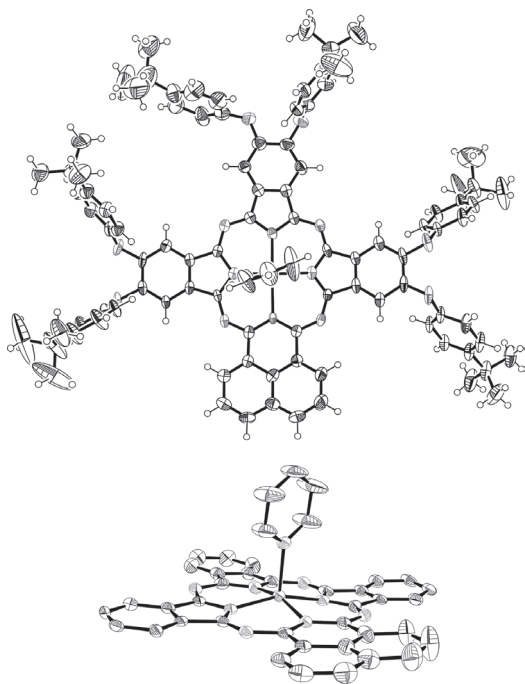
**Figure 5.** X-Ray crystal structure of **2b**, top view (top) and side view (bottom). The thermal ellipsoids were scaled to the 50 % probability level. Hydrogen atoms and *p-tert*-butylphenoxy substituents were omitted for clarity in the side view (adapted from the reference [10] with permission from Wiley).
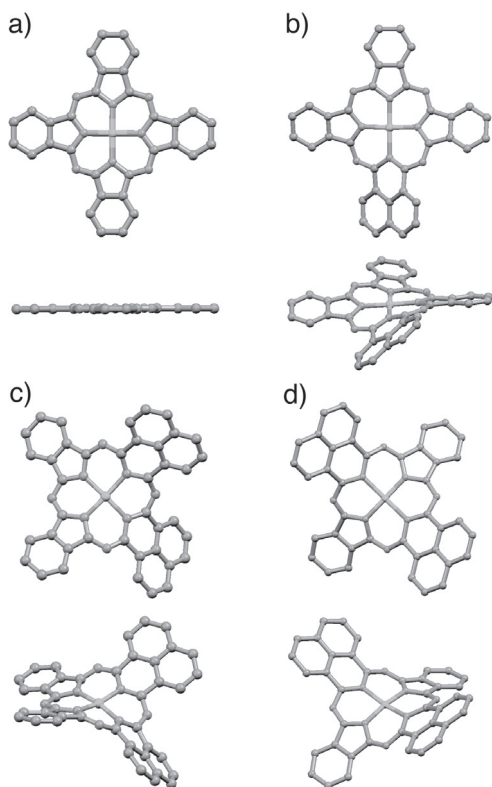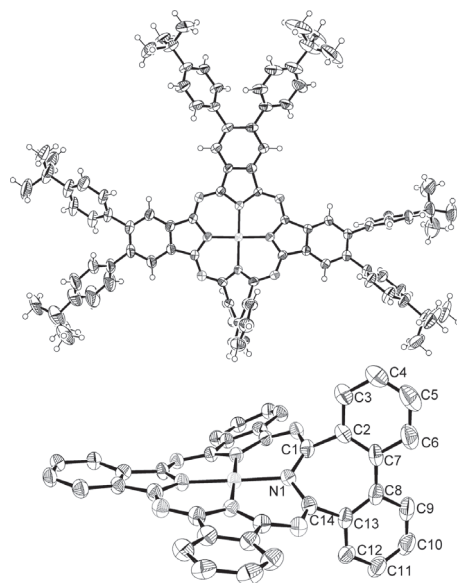


**Figure 6.** Optimized structures of model structures for a) **1a**, b) **2a**, c) **3**, and d) **4** at the B3LYP/6-31G(d) level, top view (top) and side view (bottom). Hydrogen atoms were omitted for clarity (adapted from the reference [10] with permission from Wiley).

exhibited a severely distorted structure with significant twist of the azaphenalene moiety by *ca.* 30° from the 4N mean plane. In the cases of **3** and **4**, the distortion from planarity was further enhanced, and the saddle-like conformations were observed.

Increase of the size of the inner ring unit from a six-membered ring to a seven-membered ring unit further has caused significant distortion. Almost perpendicular arrangement of the azepine moiety from the 4N mean plane was observed in the crystal structure of **5b**, while the rest of molecule has possessed a slightly distorted ruffle conformation (Figure 7).[11a] Similar structures were also predicted for **6** and **7** based on the DFT calculations at the B3LYP/6-31G(d) level (Figure 8).[11b] The single bond natures of the C1–C2 and C13–C14 bonds in **5b** have inferred rather small contribution of the azepine moiety to the overall macrocyclic conjugated system due to the large twist at these positions.

Depending on the inner ring units and molecular symmetries, the core-modified Pcs have exhibited Pc-like intense Q band absorption in the visible and near infrared



**Figure 7.** X-Ray crystal structure of **5b**, top view (top) and side view (bottom). The thermal ellipsoids were scaled to the 50 % probability level. Hydrogen atoms and *p-tert*-butylphenyl substituents were omitted for clarity in the side view (adapted from the reference [11a] with permission from The Royal Society of Chemistry).
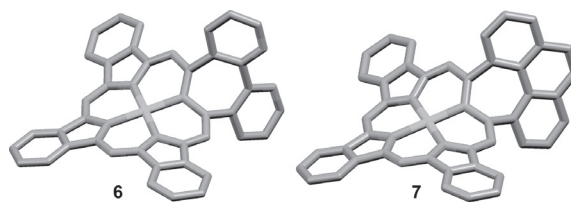


**Figure 8.** Optimized structures of model structures for **6** (left) and **7** (right) at the B3LYP/6-31G(d) level. Hydrogen atoms were omitted for clarity (reproduced from the reference [11b] with permission from Elsevier).

regions. Considering that the main absorption of nonaromatic hemiporphyrazines appears in much shorter wavelength region,[7-9] it is implied that these core-modified Pcs retain the aromatic conjugated system of Pc, which was also supported by the chemical shifts of the peripheral protons of these compounds in the ^{1}H NMR spectra. According to the Gouterman's four orbital theory,[19] the Q bands consist of transitions from the HOMO to the degenerate LUMOs. Therefore, optical and electrochemical studies can give an insight into changes in the relative energy levels of these MOs upon core-modification.

APPcs (**2–4**) have exhibited significant red-shift of the Q bands compared to those of regular Pcs at *ca.* 670 nm (Figure 9).[10] The degree of the red-shift have depended on the number of six-membered ring units. In addition to the absorption spectra, magnetic circular dichroism (MCD) spectra were also measured because this spectroscopy provides information such as the orbital degeneracies that cannot readily be deduced from other spectroscopies.[2,20] Generally characteristic spectral patterns referred to as a Faraday *A* term and Faraday *B* term are observed for the Soret and Q band absorption of porphyrins, phthalocyanines, and their related analogues. A Faraday *A* term, a derivative-shaped signal with an inflection point at the absorption maximum, and a couple of Faraday *B* terms, a set of trough and peak with Gaussian-type shapes corresponding closely to the absorption maxima, are observed when the excited states are degenerate and non-degenerate, respectively. The Faraday *B* terms corresponding to the split Q bands observed for **2a**, **2b**, and **4** in the MCD spectra were indicative of non-degeneracy of the LUMO and LUMO+1. In contrast, **3** has showed a single, broad Q band at 871 nm. The pseudo

Faraday *A* term of this Q band absorption in the MCD spectrum have indicated that the excited states of **3** were accidentally nearly-degenerate.

The cyclic voltammetry measurements on APPcs have revealed that the sizable negative shift of the first oxidation potentials from **2a** (0.085 V *vs.* Fc/Fc[+]) to **3** (−0.13 V) and further to **4** (−0.23 V), while the shift of the first reduction potential was modest (**2a**: −1.35 V, **3**: −1.41 V, **4**: −1.28 V). These results have indicated destabilization of the HOMO energy levels as well as decrease in the HOMO-LUMO energy gaps upon increasing the number of the six-membered ring units in the core.

The DFT and time-dependent (TD) DFT calculations have supported these results of the absorption spectral and electrochemical measurements (Figure 10). In addition to the destabilization of the HOMO energy level, near-degeneracy of the LUMO and LUMO+1 of **3** and their non-degeneracy of **2a** and **4** were also well reproduced. Due to the delocalization of the LUMO and LUMO+1 along the x- and y-molecular axes in the case of fourfold symmetric Pcs, introduction of azaphenalene moieties along one direction as in the cases of **2a** and **4** have caused non-degeneracy of these orbitals. On the other hand, these orbitals of **3** were accidentally degenerate in energy due to the presence of the azaphenalene moieties on both the x- and y-directions. Changes in the energy of these frontier MOs are similar to those observed for benzene-fused low symmetry Pcs.[21] This clearly indicates that the electronic structures of APPcs fall into the same category of the Pc-like aromatic conjugated systems.

In contrast to the red-shift of the Q band of APPcs, AZPPcs **5a** and **5b** have exhibited significantly split Q bands, which has appeared in both shorter and longer wavelength
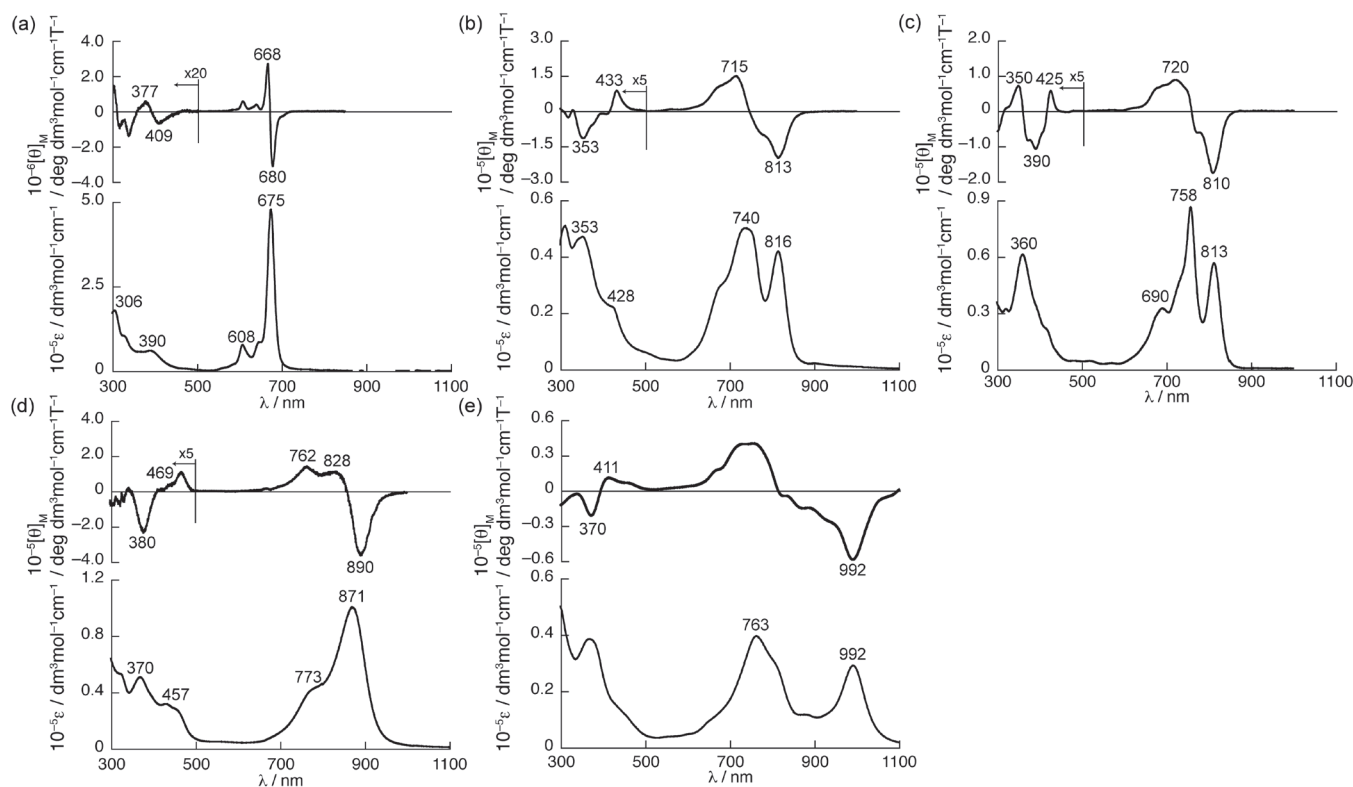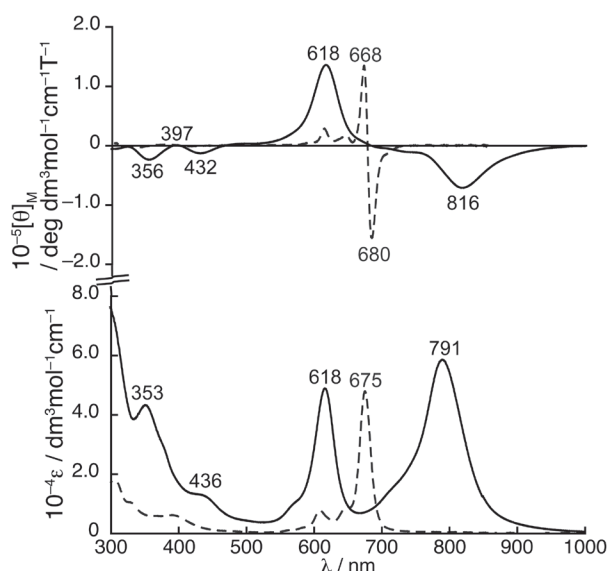


**Figure 9.** UV/Vis/NIR absorption (bottom) and MCD (top) spectra of a) **1a**, b) **2a**, c) **2b**, d) **3**, and e) **4** in CHCl₃ (reproduced from the reference [10] with permission from Wiley).
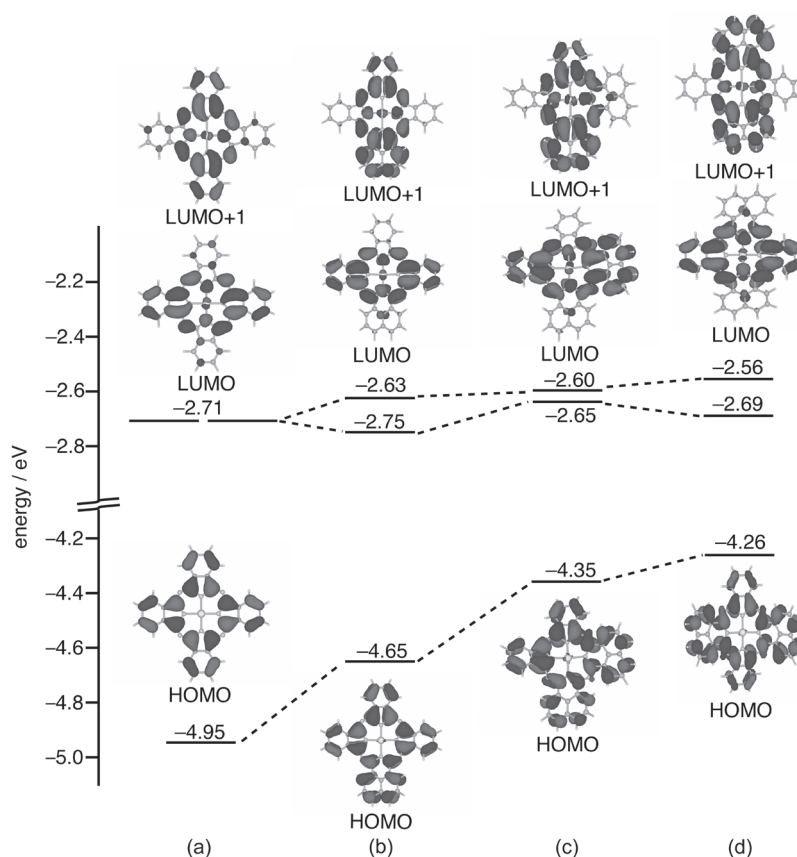
**Figure 10.** Partial frontier MO diagram of model structures of a) **1a**, b) **2a**, c) **3**, and d) **4** (adapted from the reference [10] with permission from Wiley).

regions compared to those of regular Pcs (Figure 11).[11a] With respect to the split Q bands, Faraday *B* terms were observed in the MCD spectra. Almost no alteration in the



**Figure 11.** UV/Vis/NIR absorption (bottom) and MCD (top) spectra of **5a** in CHCl$_3$. The normalized UV/Vis absorption and MCD spectra of Pc with the same substituents (**1a**) in CHCl$_3$ is shown as a reference (the intensity is shown in arbitrary units, dashed line) (reproduced from the reference [11a] with permission from The Royal Society of Chemistry).

positions and spectral morphologies of the Q band absorption was observed by changing the peripheral moieties from biphenyl to bipyridyl (**6**) and phenanthrene (**7**).[11b] This has indicated that the azepine unit was not incorporated into the macrocyclic conjugated system. The cyclic voltammetry measurement has revealed the negative and positive shifts of the first oxidation and reduction potentials, respectively, compared to those of Pc **1a**, indicating destabilization of the HOMO and stabilization of the LUMO.

In the frontier MOs based on the DFT calculation at the B3LYP/6-31G(d) level, MO coefficients could not be found on the seven-membered ring moiety due to its significant twist from the rest of the structure as observed for the crystal structure (Figure 12). These changes in the MO distribution pattern have caused the significant destabilization of the HOMO and the LUMO+1 and slight stabilization of the LUMO. The TDDFT calculation has well reproduced the observed significantly splitting of Q bands. These frontier MOs and the spectral morphologies of the Q bands are essentially similar to those of azachlorin-type macrocycles, indicating that the electronic structure of AZPPc is rather similar to azachlorin[22] than Pc.

## Core-Modified SubPcs

The successful synthesis of core-modified Pcs with six-membered and seven-membered ring units further has motivated us to apply this synthetic strategy
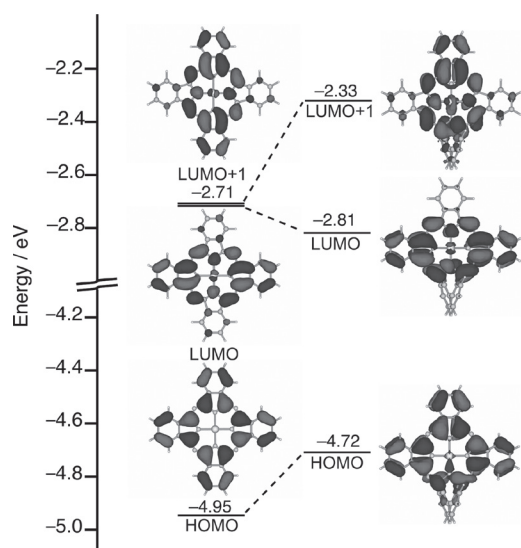
**Figure 12.** Partial frontier MO diagram of model structures of **1a** (left) and **5a** (right) (adapted from the reference [11a] with permission from The Royal Society of Chemistry).
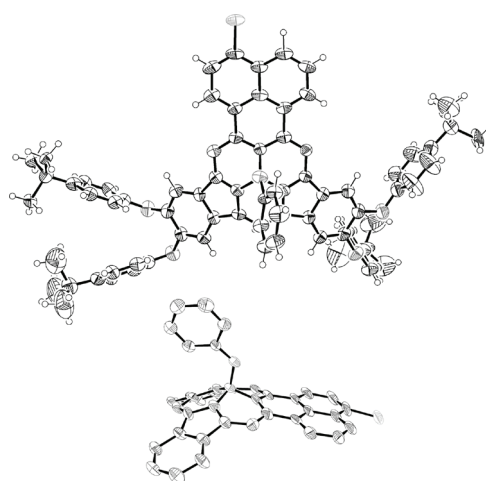


**Figure 13.** X-ray crystal structure of **8**, top view (top) and side view (bottom). The thermal ellipsoids were scaled to the 50 % probability level. Hydrogen atoms and *p-tert*-butylphenoxy substituents were omitted for clarity in the side view (adapted from [12] with permission from Wiley).

to the synthesis of SubPc, a ring contracted analogue of Pc.[23] In the presence of boron trichloride as a template, a mixed condensation reaction of *o*-phthalonitrile and 1,8-naphthalenedicarbonitrile[15] has provided core-modified SubPc analogues with a six-membered ring unit in 1.6 % yield (**8**, subazaphenalenephthalocyanine (SubAPPc)) (Scheme 3).[12,14] Based on the mass and $^1$H NMR spectra, 4- or 5-position of the peripheral naphthalene moiety was chlorinated. The structure was unambiguously elucidated by the X-ray crystallographic analysis (Figure 13). The peripheral chloride was disordered at the 4- and 5-positions with 7:3 occupancy in one of the enantiomers. The distortion of the azaphenalene unit from the mean plane by 23° is smaller than **2a** mainly due to release of the steric strain by the bowl-shaped structure.
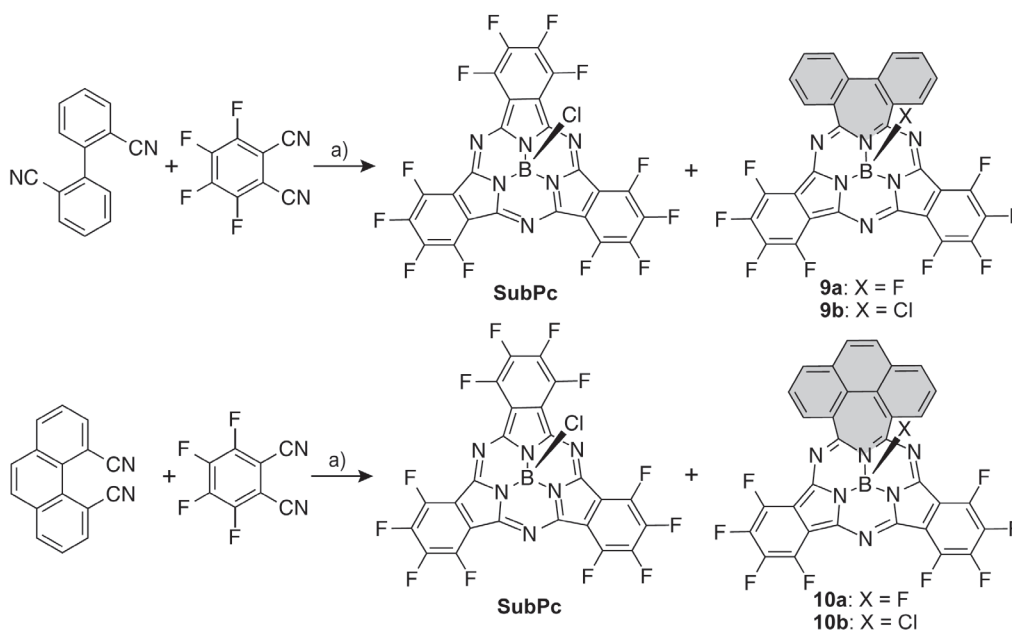
The seven-membered-ring-containing SubPc analogues **9a** and **10a** were also successfully synthesized in 9.1 and 9.8 % yields, respectively, using 2,2'-biphenyldicarbonitrile[17] and 4,5-phenantherenedicarbonitrile[18] instead of 1,8-naphthalenedicarbonitrile (Scheme 4).[13,14]

To our surprise, however, mixed condensation reactions with tetrafluorophthalonitrile can only provide these

target core-modified compounds. This unique reactivity was explained by the $^{19}$F NMR spectra of **9a** and **10a** as well as the single crystal structure of **9a** (Figure 14). The crystal structure has possessed a fluorine atom at the axial position of the boron at the center, which was also confirmed by the a quartet $^{19}$F signal at –149.6 ppm for **9a** and –149.4 ppm for **10a** due to the characteristic B-F coupling in the $^{19}$F NMR spectra. Generally SubPc can be obtained as an axially chloro-substituted species when boron trichloride is used as a template. The MALDI-TOF mass spectra of the reaction mixture have demonstrated the presence of the axially-chloro-substituted species, **9b** and **10b**, but the major molecular ion peaks have corresponded to the fluoro-substituted species. Only **9a** and **10a** were obtained due to decomposition of **9b** and **10b** during chromatographic separation (silica gel). A control experiment using *o*-phthalonitrile instead of tetrafluorophthalonitrile provided no core-modified SubPc species. The origin of the fluorine axial ligand can, therefore, be assigned to tetrafluorophthalonitrile. Although the reaction mechanism of formation of the axially fluorinated species is still unclear, one plausible explanation would be a slight change in the Lewis acidity of the central boron
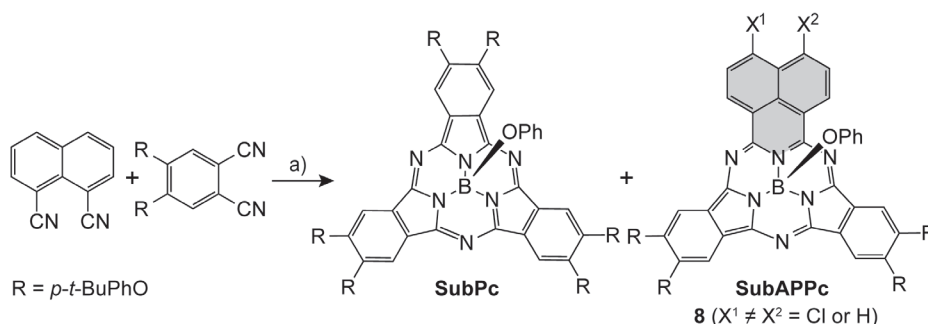


**Scheme 3.** Synthesis of subazaphenalenephthalocyanine (SubAPPc **8**). Conditions: a) 1) BCl$_3$, 1-chloronaphthalene, 190 °C; 2) phenol, 120 °C.

**Scheme 4.** Synthesis of seven-membered-ring-containing SubPcs **9a** and **10a**. Conditions: a) BCl$_3$, 1-chloronaphthalene, 180 °C.

atom upon core-modification, which are caused by much shallower bowl-shaped structures (SubPcs: 0.59~0.66 Å, **9a**: 0.58 Å, **10a**: 0.57 Å) and planar coordination geometry around the boron atom (sum of the N-B-N angles; SubPcs: 308~316°, **9a**: 317.5°, **10a**: 319.9°).[12,13,23]

Another intriguing structural feature of **9a** and **10a** was helical arrangement of the biphenyl and phenanthrene moieties. In the crystal structure of **9a**, enantiomers with *P* and *M* helicity have alternatively stacked to form one-dimensional column (Figure 14).[13] Despite the asymmetric structure of **9a** in the crystal structure and putative asymmetric structure of **10a**, the $^1$H NMR spectra of these compounds have exhibited a symmetric pattern of peripheral proton signals at room temperature, indicating a dynamic exchange between the *P* and *M* enantiomers. Upon lowering

temperature, the proton signals of **9a** became coalesced at −40 °C, and then six peaks appeared at −80 °C in CD$_2$Cl$_2$ because the fluttering motion of the biphenyl unit was thermally suppressed at this temperature. Based on the coalescence temperature, the activation energy of **9a** was estimated to be 10.7 kcal·mol$^{-1}$ at −40 °C, which is similar to the rotation barrier of propyl-bridged biphenyl derivatives. [24] In contrast, even at −80 °C the $^1$H NMR spectrum of **10a** has showed similar symmetric signal pattern as observed at room temperature. This is probably due to the smaller activation energy arising from the fused structure of the phenanthrene moiety. The $^1$H, $^1$H-COSY experiment and theoretical NMR calculations using DFT method at the B3LYP/6-31G(2d,p) level let us assign the proton signals of **9a** at 7.78 and 8.07 ppm at −80 °C to the biphenyl protons at
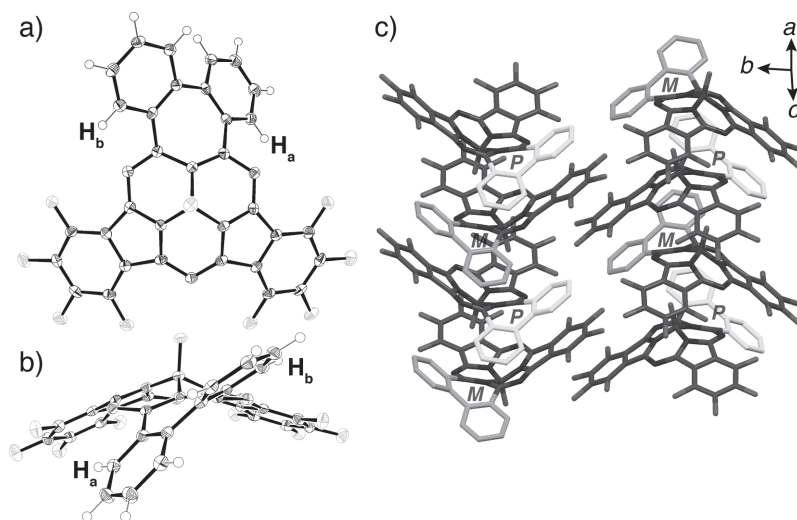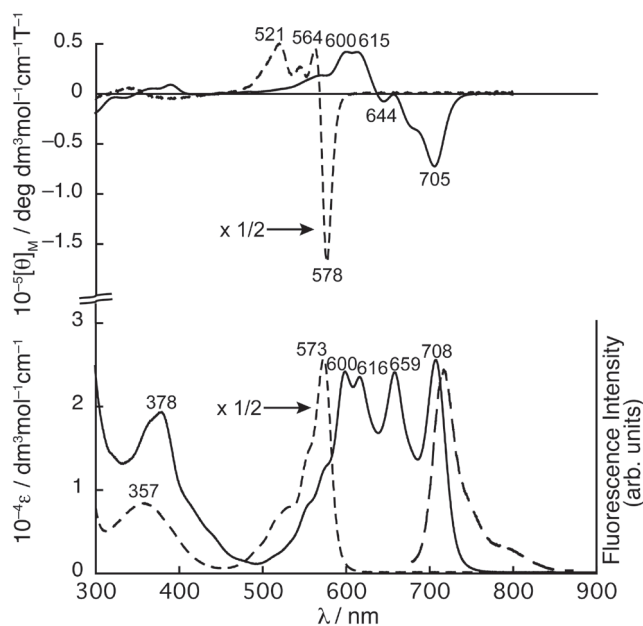


**Figure 14.** X-ray crystal structure of **9a**, a) top view, b) side view, and c) packing diagram. The thermal ellipsoids were scaled to the 50 % probability level. In the packing diagram, the biphenyl units of the *P* and *M* enantiomers are highlighted (adapted from the reference [13] with permission from Wiley).
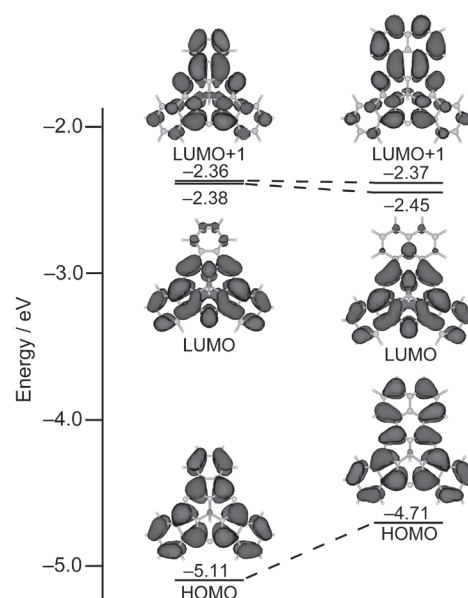
the convex (H$_b$) and concave (H$_a$) sides, respectively (Figure 14). Considering the similar distances of these protons either from the center, or the periphery of the molecule, the downfield shift of H$_a$ can be ascribed to the larger deshielding diatropic ring-current effect arising from the concave surface relative to the convex surface. Recently Torres and co-workers have also reported the difference in the ring current effects between the convex and concave surfaces.[25] Since the electronic structures of curved π-conjugated systems, as exemplified by fragmentary structures of fullerene and carbon nanotubes[26] has recently been attracting much attention, SubPc and its analogues can be suitable probe molecules for that purpose.

The core-modification of SubPc have also caused changes in absorption spectral morphologies and shift of the Q bands relative to the regular SubPc, which are similar to those observed in the cases of the core-modified Pcs. SubAPPc **8** has exhibited red-shift of the Q bands with complex splitting due to the presence of the intense vibronic bands (Figure 15).[12] The MCD spectrum has shown the Faraday *B* terms of the Q bands, indicative of the non-degenerate excited states. Band deconvolution analysis of the absorption and MCD spectra enabled assignment of the split Q$_{00}$ bands at 708 and 659 nm. Similar to the changes in the energy of the frontier MOs observed for APPcs with respect to regular Pcs, destabilization of the HOMO and non-degeneracy of the LUMO and LUMO+1 were theoretically predicted based on the DFT calculations at B3LYP/6-31G(d) level (Figure 16). The TDDFT calculation has also supported the splitting nature of the Q bands for **8**.

**9a** and **10a** both have exhibited the split of Q bands in the shorter and longer wavelength regions relative to the single Q band of regular SubPc (Figure 17).[13] The Faraday *B* terms of the Q bands in the MCD spectra were indicative of
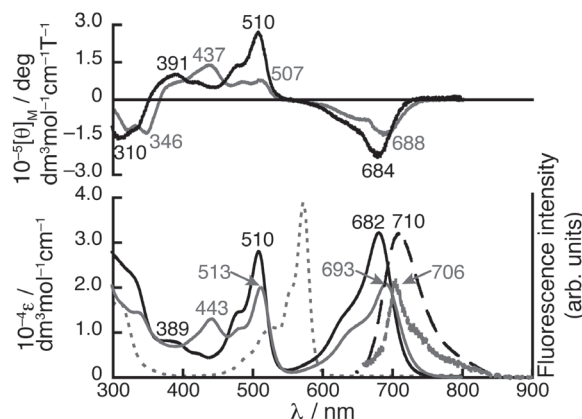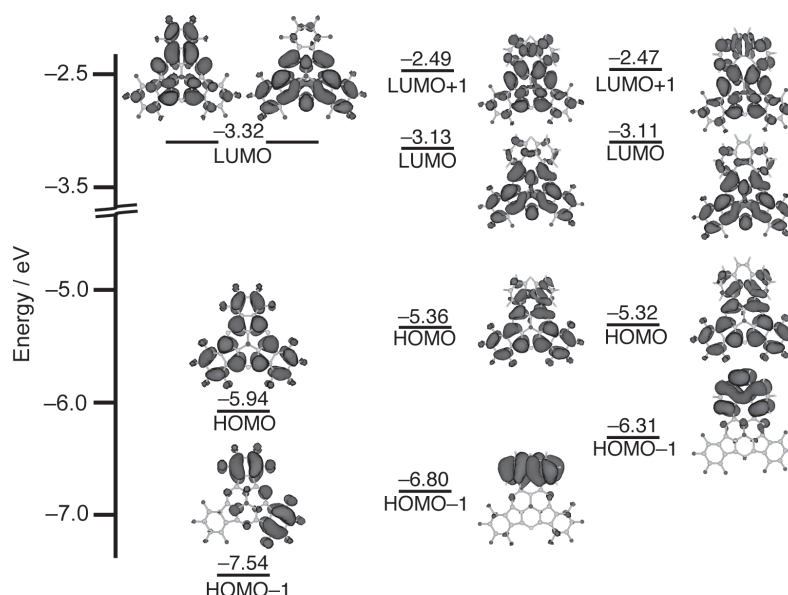


**Figure 16.** Partial frontier MO diagram of model structures of SubPc (left) and **8** (right) (adapted from the reference [12] with permission from Wiley).

the non-degenerate excited states, which were also confirmed by the DFT and TDDFT calculations. The changes in the frontier MO diagram upon core-modification and the spectral morphologies in the Q band regions have appeared to be similar to those of AZPPc. Delocalization of the MO over the molecules, however, has implied that the azepine moiety was incorporated into the conjugated system of these molecules to some extent, which is different from AZPPcs, probably due to the smaller torsion angle of the biphenyl and phenanthrene moieties (Figure 18). A characteristic intramolecular charge-transfer (CT) transition from the HOMO–1, which is localized on the biphenyl and phenanthrene moieties, to the LUMO was also observed at 389 nm for **9a** and at 443 nm for



**Figure 15.** UV/Vis absorption (bottom) and MCD (top) spectra of **8** (solid line) and SubPc with the same substituents as a reference (dashed line) in CHCl$_3$, and the fluorescence spectrum of **8** (bottom, long dashed line) (reproduced from the reference [12] with permission from Wiley).



**Figure 17.** UV/Vis absorption (bottom, solid lines), MCD (top), and fluorescence spectra (bottom, dashed lines) of **9a** (black) and **10a** (gray) in CHCl$_3$. The normalized UV/Vis absorption spectrum of SubPc with the same substituents in CHCl$_3$ is shown as a reference (the intensity is shown in arbitrary units; bottom, grey dotted line) (reproduced from the reference [13] with permission from Wiley).

**Figure 18.** Partial frontier MO diagram of model structures of SubPc (left), **9a** (middle), and **10a** (right) (reproduced from the reference [13] with permission from Wiley).

**10a**. In the case of **10a**, the intramolecular CT band was red-shifted and more clearly observed due to the destabilization of the HOMO–1.

## Conclusions

In summary, the novel core-modification strategy using dinitrile derivatives bearing nitrile groups not with a 1,2-relationship, but with a 1,3- or 1,4-relationship was proved to be effective, and core-modified Pcs and SubPcs with six- and seven-membered ring units were successfully synthesized. Upon core-modification the electronic structures and the concomitant optical and electrochemical properties were significantly altered. Incorporation of the six-membered ring units has caused the red-shift of the Q band absorption, and its splitting depending on the number and positions of the six-membered ring units. This result indicates that these core-modified Pcs and SubPcs basically retain the original electronic structures of Pcs and SubPcs. In contrast, the electronic structures have changed to the azachlorin type upon introduction of the seven-membered ring units due to the significant twist of these moieties from the main conjugated systems. Considering that Pc and SubPc analogues have been investigated as functional materials, intense absorption in the visible and near infrared regions, and facile control of the absorption wavelengths achieved by the core-modification are one of the important synthetic strategy in the Pc and SubPc chemistry, which is being further pursued in our laboratory.

## References

1. (a) Braun A., Tscherniac J. *Chem. Ber.* **1907**, *40*, 2709–2714; (b) Dandridge A.G., Drescher H.A., Thomas J. *GB Patent*, 322169, **1928**.

2. *Phthalocyanines: Properties and Applications*, Vol. 1–4 (Leznoff C.C., Lever A.B.P., Eds.), Wiley-VCH: New York, **1989-1996**.

3. *The Porphyrin Handbook,* Vol. 15-20 (Kadish K.M., Smith K.M., Guilard R., Eds.), Academic Press: San Diego, **2003**.

4. McKeown N.B. *Phthalocyanine Materials: Synthesis, Structure and Function*. Cambridge: Cambridge University Press, **1998**.

5. Kobayashi N., Fukuda T. Recent Progress in Phthalocyanine Chemistry: Synthesis and Characterization. In: *Functional Dyes* (Kim S., Ed.), Oxford: Elsevier, **2006**, pp. 1–45.

6. (a) Lash T.D. Carbaporphyrins and Related Systems. Synthesis, Characterization, Reactivity and Insights into Porphyrinoid Aromaticity. In: *Handbook of Porphyrin Science*, Vol. 16 (Kadish K.M., Smith K.M., Guilard R., Eds.), Singapore: World Scientific Publishing, **2012**, pp. 1–329; (b) Pawlicki M., Latos-Grażyński L. Carbaporphyrinoids – Synthesis and Coordination Properties. In: *Handbook of Porphryin Science*, Vol. 2 (Kadish K.M., Smith K.M., Guilard R., Eds.), Singapore: World Scientific Publishing, **2010**, pp. 103–192; (c) Stępień M., Latos-Grażyński L. *Acc. Chem. Res.* **2005**, *38*, 88–98.

7. (a) Elvidge J.A., Linstead R.P. *J. Chem. Soc.* **1952**, 5008–5012; (b) Clark P.F., Elvidge J.A., Linstead R.P. *J. Chem. Soc.* **1954**, 2490–2497.

8. (a) Fernández-Lázaro F., Torres T., Hauschel B., Hanack M. *Chem. Rev.* **1998**, *98*, 563–575; (b) Rodríguez-Morgade M.S., De La Torre G., Torres T. Design and Synthesis of Low-Sym-

metry Phthalocyanines and Related Systems. In: *The Porphyrin Handbook*, Vol. 15 (Kadish K.M., Smith K.M., Guilard R., Eds.), San Diego: Academic Press, **2003**, pp. 125–160.

9. Ziegler C.J. The Hemiporphyrazines and Related Systems. In: *Handbook of Porphyrin Science*, Vol. 17 (Kadish K.M., Smith K.M., Guilard R., Eds.). Singapore: World Sceintific Publishing, **2012**, pp. 113–238.

10. Shimizu S., Zhu H., Kobayashi N. *Chem. Eur. J.* **2010**, *16*, 11151–11159.

11. (a) Shimizu S., Zhu H., Kobayashi N. *Chem. Commun.* **2011**, *47*, 3072–3074; (b) Shimizu S., Uemura K., Zhu H., Kobayashi N. *Tetrahedron Lett.* **2012**, *53*, 579–581.

12. Zhu H., Shimizu S., Kobayashi N. *Angew. Chem. Int. Ed.* **2010**, *49*, 8000–8003.

13. Shimizu S., Nakano S., Kojima A., Kobayashi N. *Angew. Chem. Int. Ed.* **2014**, *53*, 2408–2412.

14. Shimizu S. Kobayashi N. *Chem. Commun.* **2014**, *50*, 6949–6966.

15. Qian X. H., Xiao Y. *Tetrahedron Lett.* **2002**, *43*, 2991–2994.

16. Kobayashi N., Sasaki N., Konami H. *Inorg. Chem.* **1997**, *36*, 5674–5675.

17. Ege G., Beisiegel E. *Synthesis* **1974**, 22–23.

18. Baxter P.N.W., Connor J.A., Povey D.C., Wallis J.D. *Chem. Commun.* **1991**, 1135–1137.

19. (a) Gouterman M. *J. Chem. Phys.* **1959**, *30*, 1139–1161; (b) Gouterman M. *J. Mol. Spectrosc.* **1961**, *6*, 138–163.

20. (a) Kobayashi N., Muranaka A., Mack J. *Circular Dichroism and Magnetic Circular Dichroism Spectroscopy for Organic Chemists*. UK: Royal Society of Chemistry, **2012**. 216 p.; (b) Mack J., Stillman M.J., Kobayashi N. *Coord. Chem. Rev.* **2007**, *251*, 429–453.

21. (a) Fukuda T., Makarova E.A., Luk'yanets E.A., Kobayashi N. *Chem. Eur. J.* **2004**, *10*, 117–133; (b) Kobayashi N., Fukuda T. *J. Am. Chem. Soc.* **2002**, *124*, 8021–8034; (c) Kobayashi N., Miwa H., Nemykin V.N. *J. Am. Chem. Soc.* **2002**, *124*, 8007–8020; (d) Miwa H., Ishii K., Kobayashi N. *Chem. Eur. J.* **2004**, *10*, 4422–4435.

22. (a) Linstead R.P., Whalley M. *J. Chem. Soc.* **1952**, 4839–4846; (b) Mani N.S., Beall L.S., White A.J.P., Williams D.J., Barrett A.G.M., Hoffman B.M. *Chem. Commun.* **1994**, 1943–1944; (c) Montalban A.G., Lange S., Beall L.S., Mani N.S., Williams D.J., White A.J.P., Barrett A.G.M., Hoffman B.M. *J. Org. Chem.* **1997**, *62*, 9284–9289; (d) Fukuda T., Kobayashi N. *Dalton Trans.* **2008**, 4685-4704; (e) Nemykin V.N., Polshyna A.E., Makarova E.A., Kobayashi N., Lukyanets E.A. *Chem. Commun.* **2012**, *48*, 3650–3652; (f) Sugita I., Shimizu S., Fukuda T., Kobayashi N. *Tetrahedron Lett.* **2013**, *54*, 1599–1601.

23. (a) Claessens C.G., González-Rodríguez D., Torres T. *Chem. Rev.* **2002**, *102*, 835–853; (b) Claessens C.G., González-Rodríguez D., Rodríguez-Morgade M.S., Medina A., Torres T. *Chem. Rev.* **2014**, *114*, 2192–2277.

24. Rotzler J., Gsellinger H., Neuburger M., Vonlanthen D., Haussinger D., Mayor M. *Org. Biomol. Chem.* **2011**, *9*, 86–91.

25. (a) Caballero E., Fernández-Ariza J., Lynch V.M., Romero-Nieto C., Rodríguez-Morgade M.S., Sessler J.L., Guldi D.M., Torres T. *Angew. Chem. Int. Ed.* **2012**, *51*, 11337–11342; (b) González-Rodríguez D., Carbonell E., Rojas G.D., Castellanos C.A., Guldi D.M., Torres T. *J. Am. Chem. Soc.* **2010**, *132*, 16488–16500; (c) González-Rodríguez D., Carbonell E., Guldi D.M., Torres T. *Angew. Chem. Int. Ed.* **2009**, *48*, 8032–8036; (d) González-Rodríguez D., Torres T., Herranz M.A., Echegoyen L., Carbonell E., Guldi D.M. *Chem. Eur. J.* **2008**, *14*, 7670–7679; (e) Iglesias R.S., Claessens C.G., Torres T., Rahman G.M.A., Guldi D.M. *Chem. Commun.* **2005**, 2113–2115; (f) González-Rodríguez D., Torres T., Guldi D.M., Rivera J., Herranz M.A., Echegoyen L. *J. Am. Chem. Soc.* **2004**, *126*, 6301–6313.

26. *Fragments of Fullerenes and Carbon Nanotubes: Designed Synthesis, Unusual Reactions, and Coordination Chemistry.* (Petrukhina M.A., Scott L.T., Eds.), Hoboken: Wiley&Sons, Inc., **2011**. 413 p.